Nuclear Magnetic Resonance

Joseph Mattern
Partner: Albert Guo*
Stony Brook University
(Dated: June 21, 2020)

We used Teachspin's pulsed nuclear magnetic resonance apparatus to determine the relaxation times of mineral oil and glycerin. Specifically, values for their spin-lattice (T_1) and spin-spin (T_2) relaxation times, as well as their components, $T_2^{'}$, T_2^{*}, and $T_2^{''}$, were successfully calculated and determined. T_2 times were found to be 60(10)μs and 50(3)μs for mineral oil and glycerin, respectively. The T_1 times were calculated to be 25.69(4)ms and 59.6(3)ms using our most reliable method. Our calculations resulted in an unusualy high $T_2^{''}$ which is uncommon when examining liquids.

I. INTRODUCTION

Nuclear magnetic resonance (NMR) is a spectroscopic method, which allows the study of interactions between atomic nuclei and magnetic fields. This technique is used throughout the sciences, and it is most common in medicine, where it is used as a non-invasive scanning method for sensitive parts of the body in Magnetic Resonance Imaging (MRI).

In pulsed NMR (PNMR), nuclei subjected to a strong external magnetic field are perturbed with a weak oscillating magnetic field in the form of a radio frequency (RF) wave. Depending on the nuclei, the magnetic field, and the RF frequency and pulse time, a collective spin response of the system can be observed and measured, in the form of a precessing net magnetization at the frequency of a resonant RF signal [5].

In this experiment, the characteristic relaxation times T of mineral oil and glycerin were determined using PNMR, on their covalently bonded hydrogen molecules, which act close to free protons [6].

A. Theory

When a nucleus with intrinsic magnetic moment μ is placed in a strong static field $B_0\hat{\mathbf{z}}$, nuclear spins will align in the $\hat{\mathbf{z}}$ direction parallel to the field, and the energy levels of the spectrum will then be quantized to a spacing of $\Delta E = \hbar\gamma B_0$, where $\gamma = \mu/(J\hbar)$ is the gyromagnetic ratio, which gives the magnetic moment to angular momentum ratio with J being the spin of the nucleus.

In this static case, the magnetization can be calculated by the population difference of up and down spins, respectively n_+ and n_-, so that

$$M_z = M_0 = \gamma\hbar\frac{(n_+ - n_-)}{2}.$$

This is the z component of the magnetization vector of the material, neglecting the effect of the interaction between the static field and the spins.

Using Bloch's equations [3] for simple relaxational dynamics, the evolution of a perturbed magnetization in the presence of a static field can be described, in a rotating frame of angular frequency ω, as

$$\begin{aligned}\frac{dM_z}{dt} &= -\gamma M_y B_0 + (M_0 - M_z)/T_1 \\ \frac{dM_x}{dt} &= \gamma M_y b_0 - M_x/T_2 \\ \frac{dM_z}{dt} &= \gamma(M_z B_1 - M_x b_0) - M_y/T_2,\end{aligned} \tag{1}$$

where $b_0 = B_0 - \omega/\gamma$, and with the RF field B_1 along the x-direction of the rotating frame. The above equations also apply for PNMR, such that in perturbing the spin system with an oscillating magnetic field at the resonant frequency $\omega = \gamma B_0$, $b_0 = 0$. At times much shorter than T_1 or T_2, the Bloch equations reduce to describing a rotation of $\mathbf{M}$ about the x-axis. When pulsed for just the right duration, the angle of rotation can be made to be exactly 90°, corresponding to a "$\frac{\pi}{2}$"-pulse, or exactly opposite their original direction, corresponding to a "π"-pulse.

After the event of a $\frac{\pi}{2}$ pulse the spins, and thus the net magnetization, precess about the z-axis as the perpendicular magnetization returns to equilibrium. Because the magnetization vector has non zero components in the xy-plane, the precessing magnetization induces an oscillating voltage in the pickup coil in the apparatus. This observable signal is called the free induction decay (FID) [4].

The free induction decay signal is best explained by Bloch's equation for M_{xy} neglecting the the interaction between the static field and the nuclear spins, with the solution

$$M_{xy}(t) = M_{xy}(0)e^{-t/T_2}. \tag{2}$$

The FID amplitude signal is proportional to the perpendicular component of the magnetization, with a decay time of T_2.

* Joseph.mattern@stonybrook.edu ; Albert.guo@stonybrook.edu

Due to local inhomogeneities in the magnetic field B_0, the spins do not all precess at the same rate and dephase over time. Due to this this broadening, T_2 can be broken down into two components,

$$\frac{1}{T_2} = \frac{1}{T_2^*} + \frac{1}{T_2^{'}}, \tag{3}$$

where T_2^* is the characteristic time for the spins to dephase, representing the loss of coherence due to inhomogeneous broadening, and $T_2^{'}$ is the intrinsic spin relaxation time, representing the decay of M_{xy} due to spin interactions (whether they be spin-spin or spin-sample interactions).

$T_2^{'}$ can be further broken down into

$$\frac{1}{T_2^{'}} = \frac{1}{T_2^{"}} + \frac{1}{2T_1}, \tag{4}$$

where $T_2^{"}$ is the relaxation time due to interactions between the spins themselves, and T_1 is the relaxation time due to the interaction between the spins and the rest of the sample. T_1 is called the spin-lattice relaxation time, and it is the decay time in the evolution of the magnetization as it returns to thermal equilibrium, which can be seen in Bloch's equation for M_z while neglecting B_1, which has solution

$$M_z(t) = M_z(0)(1 - e^{-t/T_1}). \tag{5}$$

II. PROCEDURE

In this experiment, a TeachSpin PS1-A PNMR spectrometer was used. A sketch and picture of the experiment setup can be seen in Figs. 1 and 2. The static B_0 field is provided by two permanent magnets (see Fig. 1b), while the RF signal is provided by transmitter coils (wound as Helmholtz coils), which take in an amplified RF signal from the RF oscillator and produces a field B_1 that rotates the spins out of equilibrium. Only the component of the magnetization perpendicular to B_0 is actually measured: the oscillating signal from a pickup coil wound around the sample is amplified by a receiver and rectified, such that a detector sends only a positive envelope of the amplified signal to be measured by the oscilloscope. A second mixer signal, consisting of the product of the RF oscillator signal and the amplified pickup coil signal is measured alongside the detector signal, to allow tuning of the RF frequency to resonance.

A. Measuring ω

Two samples were investigated: mineral oil and glycerin. For each sample, the resonance precession frequency $\omega = \gamma B_0$ was first determined by applying a

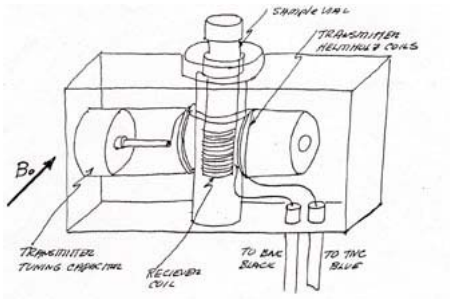

(a)

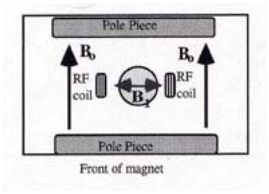

(b)

Figure 1: (a) A sketch of the receiver coil of the apparatus with a reference to the static magnetic field. A sample is placed within the receiver coil, to be perturb by a signal sent from the RF coils in (b). The transmitting tuning capacitor can be adjusted by turning or sliding rods that stick out of the bottom of the probe at the base of the magnet [1] An overhead view of the sketch shown in (b) shows B_1 in reference to B_0

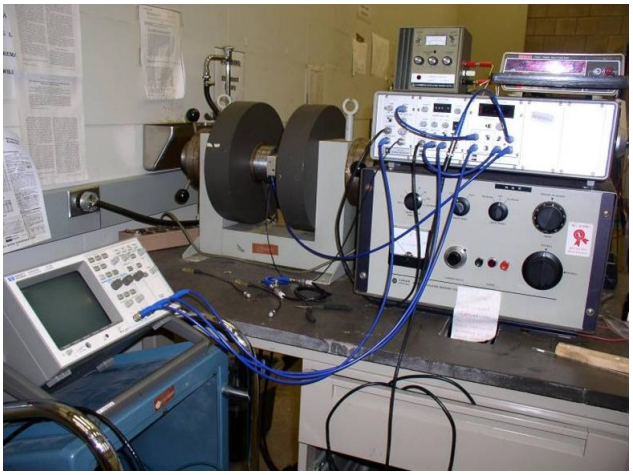

Figure 2: A picture of experiment setup, on the left, one can see the oscilloscope, followed by the two permanent magnets right behind it that provide the static magnetic field. In between those is the receiver coil that sends the signal to the electronics on the right where it is amplified and rectified, through a series of electronic procedures.

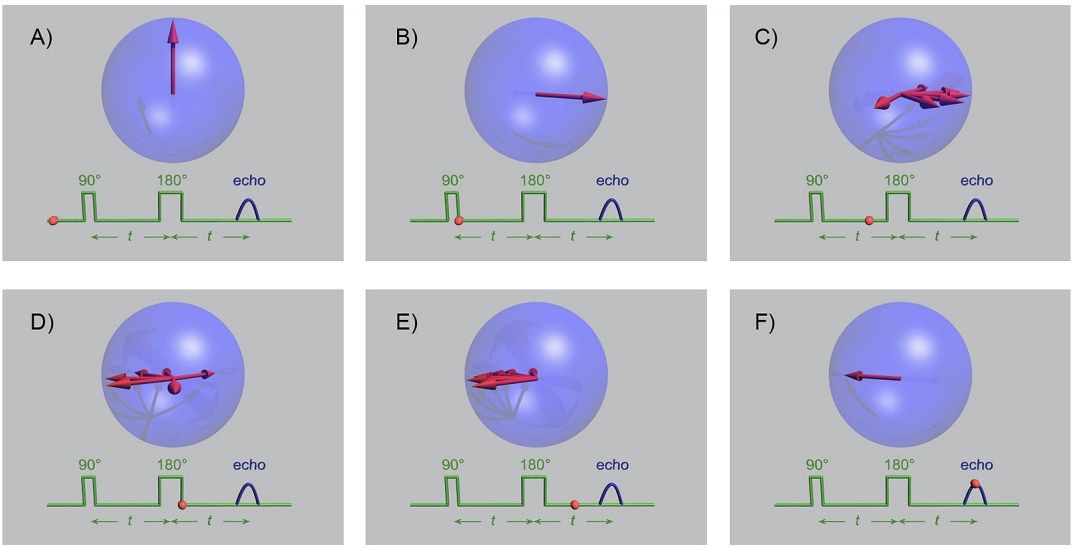

Figure 3: A step-by-step process of spin echo, first the magnetization vectors of the nuclei are aligned with the static magnetic field (A), then a $\pi/2$ pulse is applied perturbing the magnetization vector out of phase by 90 degrees (B). (C) Shows the process of dephasing due to inhomogeneity in the magnetic field causing different precession speeds. At the right time (D) a π pulse is applied flipping the orientation of the magnetization vector, so that in (E) all the varying precessions of nuclei are refocused at (F) causing an echo (Spin Echo).

$\frac{\pi}{2}$ pulse to generate an FID decay curve. The RF frequency was then tuned until the mixer output displayed no beats, indicating that the precession frequency was equal to the RF frequency. The measured (non-angular) frequencies f are shown in the second column of Table I, with an uncertainty estimated from the range of frequencies that created no beats in the mixer signal.

B. Measuring T_2

From Eq. 2, T_2 is the decay constant of the FID decay, which was found by simply fitting an exponential decay to the decay portion of the FID signal (see Figs. 6).

C. Measuring $T_2^{'}$

$T_2^{'}$ can be experimentally measured by introducing the π pulse. After a $\pi/2$ pulse that rotates the magnetization perpendicular to the static field, the individual spins, initially all in phase along the magnetization, precess at different rates depending on the local magnetic field. Applying a π pulse after a time τ flips the spins 180°, reversing the angular positions of the slow and fast spins along the precession direction. A time 2τ after the initial $\frac{\pi}{2}$ pulse, the fast spins catch up to the flipped slow spins, causing all the spins to rephase, resulting in a brief refocusing of the net magnetisation as they cross each other, commonly known as the 'spin echo'. A good description can be found at [2], in Fig. 3.

By subsequently applying π pulses one after another with a time separation of 2τ, a train of spin echoes can be created, as the spins continuously rephase and dephase after each pulse. $T_2^{'}$ can be determined as the decay constant in the exponential decay of the echo amplitudes,

$$M_{\text{echo}}(t) = M(0)e^{-t/T_2^{'}}. \tag{6}$$

This spin echo method circumvents the effects of local field inhomogeneities (T_2^*), as the application of π pulses flipping the precessing spins cancels out the effects of these local inhomogeneities in the resulting echo.

For both samples, a pulse sequence consisting of a $\frac{\pi}{2}$ pulse followed by 24 π pulses was applied with $\tau = 1.0\,\text{ms}$, to create a train of 24 spin echoes. The echoes were then fitted with Gaussian functions to determine the peak amplitudes, and those amplitudes were then fitted with an exponential decay, as in Eq. 6, to determine $T_2^{'}$ (see Figs. 5). The repetition rate for both trials was 10 Hz.

D. Measuring T_1

Because our experiment only measures the perpendicular magnetization M_{xy} while T_1 is related to the evolution of M_z as it returns to equilibrium, indirect

methods have to be employed to measure T_1, two of which were investigated in this experiment.

1. Method A

Similar to creating a spin echo, this method involves applying consecutive pulses, although with a pulse sequence consisting of a π pulse followed by a $\frac{\pi}{2}$ pulse after a time τ. The π pulse flips the magnetization, after which the system evolves as usual according to the Bloch equations (1). The $\frac{\pi}{2}$ acts as a camera, snapshotting the state of M_z at a time τ along its evolution by creating a FID signal with amplitude proportional to M_z at the time of the $\frac{\pi}{2}$ pulse.

The above pulse sequence was performed for both samples at various values of τ with a repetition rate of 10 Hz, with the FID amplitudes measured and plotted versus τ. The plots were then fitted (after negating the points before the 0-crossing of M_z) with Eq. 5 to determine $T_{1,\mathrm{A}}$ (see Figs. 4a, b).

2. Method B

T_1 can also be measured by studying the FID amplitude as a function of repetition rate. A $\frac{\pi}{2}$ pulse was applied at various repetition rates for mineral oil, with the FID amplitudes measured and plotted in Fig. 4c. A simple exponential decay fit was performed, with the inverse of the time constant of the fit (since the x-axis is in Hz) as our calculated $T_{1,\mathrm{B}}$.

III. DATA AND RESULTS

Calculated relaxation times T for both mineral oil and glycerin are displayed in Table. I.

Due to significant noise from the detector, all oscilloscope captures were performed using the scope's "Average" function, which displays a moving average of the signal, based on the previous 8 triggers (up to 16 for extremely noisy signals). Only one capture was used for each data point; uncertainty in each point in the raw data from the scope capture was thus taken to be half the vertical resolution of the scope.

Curve fitting (e.g. exponential decay for data points of aggregate data) and Gaussian functions for spin echo peaks) was performed using the `curve_fit` function from Python's `scipy.optimize` package, which returns the covariance matrix of the fitted optimal parameters when uncertainties in fitted points are given as input, allowing calculation of the parameter uncertainties as simply the square root of diagonal entries of the covariance matrix.

Substance	f [MHz]	$T_{1,\mathrm{A}}$ [ms]	$T_{1,\mathrm{B}}$ [ms]	T_2 [µs]	T_2' [ms]	T_2^* [µs]	T_2'' [ms]
Mineral oil	14.842(1)	25.69(4)	27.8(1.7)	60(10)	15.5(3)	60(10)	22.2(6)
Glycerin	14.788(1)	59.6(3)	–	50(3)	53(7)	50(3)	94(21)

Table I: Measured and calculated relaxation times for mineral oil and glycerin, with measured resonant RF frequency

T_1 was found using both methods A and B for mineral oil, but because the FID signal broke down for repetition frequencies above 20 Hz with glycerin, T_1 was calculated using only method A. Plots and fits for methods A and B for both substances are shown in Fig. 4. In fitting Eq. 5 (with 2 parameters, M_0 and T_1) in method A for glycerin, the initial fit of all data points gave $T_{1,\mathrm{A}} \approx 52$ ms (see Fig. 4b, blue fit). A 10 Hz repetition rate gives a time between triggers (i.e., between π pulses) of $\Delta t = 100$ ms, so that at large τ, $(\Delta t - \tau)/T_1$ becomes on the order of 1. In other words, for the last 3 points in Fig. 4b, τ is large enough such that the π pulse of the next trigger comes after the current $\frac{\pi}{2}$ pulse in less time than T_1, which would significantly affect the FID amplitude. Another fit was performed omitting these points, giving the fit in red and the value recorded in Table I, of $T_{1,\mathrm{A}} = 59.6(3)$ms.

T_2 was found by fitting an 3-parameter exponential decay function (of the form $V(t) = ae^{-t/T_2} + b$) to the FID decay signal for each respective sample, as seen in Fig. 6. Because a simple exponential decay did not fit well for the entire decay range (from after the peak to the end) in either sample, fits were performed on sections of the FID decay while recording the fitted T_2 parameter. The displayed T_2 values in Table I are thus a rough average of the range of recorded T_2 parameters, compensated for by a large estimated variance.

T_2^* and T_2'' were calculated using their respective formulas (Eq. 3 and Eq. 4), with their uncertainties propagated using the standard formula for propagating Gaussian uncertainties.

IV. CONCLUSION

Looking at the calculated T values in Fig. I, the two values $T_{1,\mathrm{A}}$ and $T_{1,\mathrm{B}}$ for mineral oil agree with each other well up to experimental uncertainty, with a significance ratio of $|T_A - T_B| / \sqrt{\sigma_A^2 + \sigma_B^2} = 1.24$. In liquids, it is expected that $T_2' \approx 2T_1$, or equivalently by Eq. 4, that $T_2'' \approx 0$. However, in the calculated values, $T_2'/T_1 = 0.6,\ 0.8$ for mineral oil and glycerin, respectively, and calculated T_2'' values are significantly different from 0. This could be due to the effects of low motional narrowing, where the effects of diffusion are

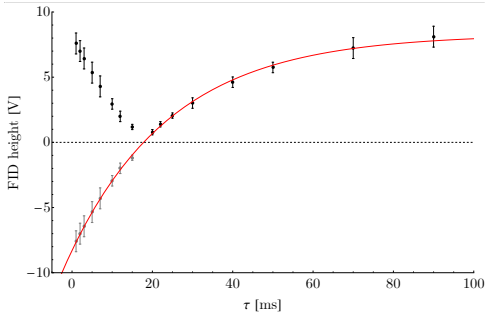

(a)

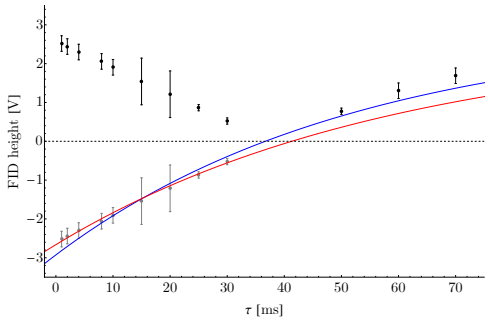

(b)

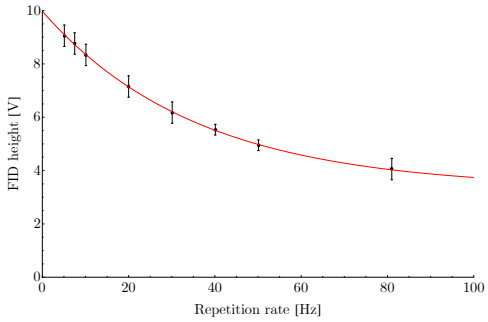

(c)

Figure 4: Fitted plots to calculate T_1 values for mineral oil ((a) & (c)) and glycerin (b) using methods A (for (a), (b)) and B (for (c)). Errors increased by factor of 10 in (a) & (b) and by factor of 5 in (c) for visibility. In (b), the red fit corresponds to fitting only the points before the crossing point of $\sim 38\,\mathrm{ms}$, while the blue fit corresponds to fitting all points. Reduced $\chi^2 = 20$ (a), 175 (b, red), 9.56 (b, blue), and 0.37 (c)

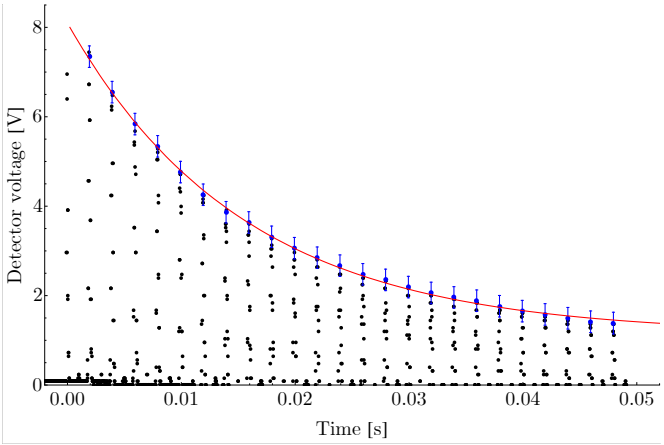

(a)

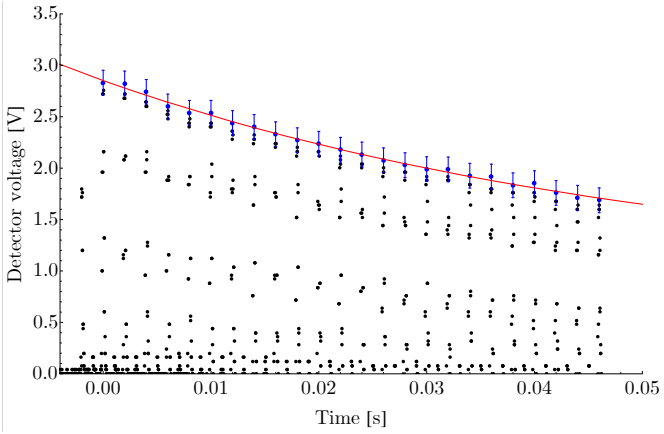

(b)

Figure 5: Spin echo sequences (from oscilloscope) for mineral oil (a) and glycerin (b), both with $\tau = 1.0\,\mathrm{ms}$ and with repetition rate of 10 Hz. Errors on points in blue (obtained from fitting Gaussian functions around each echo peak) increased by factor of 5 for visibility. Reduced $\chi^2 = 1.31$ d.o.f.= 21 (a), 1.17 d.o.f.= 21 (b).

not sufficient in either sample to suppress spin-spin interactions, i.e. $T_2^{''}$. Glycerin was observed to be more viscous than mineral oil, and thus has a higher $T_2^{''}$ than mineral oil (both its absolute value and relative value, compared to T_1 and $T_2^{'}$. Future experiments could explore the effects (or absence) of motional narrowing in various materials and liquids, in relation to their diffusion properties.

One source of systematic error is the effect that caused the observed gradual change in the resonant frequency f of the sample, on the order of roughly $10\,\mathrm{kHz\,h^{-1}}$. This could be due to the effect of resistive heating in the Helmholtz coils or somehow by conduction to the permanent magnets. The former case would affect the current through the coils and thus the generated magnetic field B_1.

Significant noise was observed in measured FID signals, especially in those with lower amplitudes, such as in measuring $T_{1,\mathrm{A}}$. Despite using the scope's "Average" function, many signals had significant fluctuations while they were captured. This is a source of statistical uncertainty that was not accounted for in this experiment, as only one capture of each signal was performed, without recording any information on the variance of those

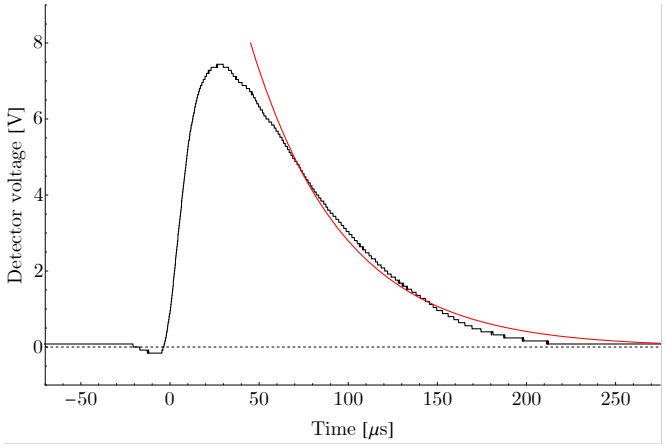

(a)

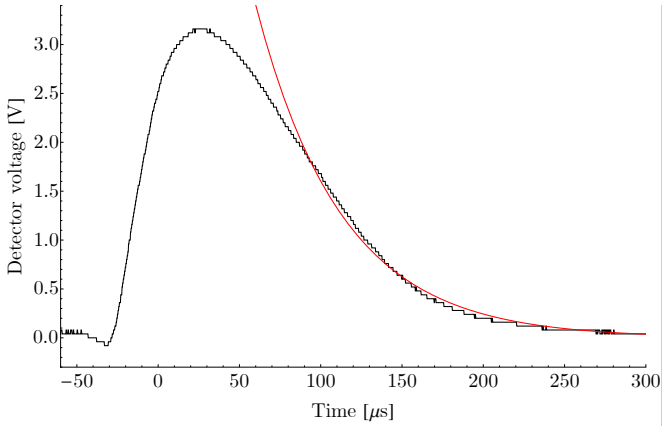

(b)

Figure 6: FID signals (from oscilloscope) after a single $\frac{\pi}{2}$ pulse for mineral oil (a) and glycerin (b), both at a repetition rate of 10 Hz, and resonant at RF frequencies 14.842 MHz and 14.788 Hz respectively ($\sigma = 0.001$ MHz). Reduced χ^2 ranges from 1-4, depending on section of FID decay fitted.

fluctuations. The uncertainty in captured signals was thus forced to be taken as the vertical resolution of the scope capture, which would at best, for more stable signals, somewhat overestimate their uncertainty, while at worst, for more noisy signals, significantly underestimate their uncertainty.

Future experiments could also involve the calculation of relaxation times of a larger variety of substances, or using PNMR on heavier nuclei rather than hydrogen.

V. CONTRIBUTIONS

' In this paper Joseph Mattern has written the thorough introduction, procedure and theoretical background of the fundamentals of Nuclear Magnetic Resonance, introducing the characteristic relaxation times and rates, that are then evaluated in the analysis. Albert Guo conducted the analysis of the data collected from the experiment obtaining the characteristic times through exponential fitting of decay parameters, using the appropriate Bloch dynamics. Credit is given to both Joseph and Albert for the formation of results from the experiment, and possible areas of error, and further studies.

[1] Anon *Things to know before you begin operating an NMR*
[2] Anon 2019 *Spin echo* Wikipedia
[3] Bloch F 1946 *Nuclear Induction* Physical Review 70 460–74
[4] Hopf F A, Shea R F and Scully, M O 1973 *Theory of Optical Free-Induction Decay and Two-Photon Superradiance*Physical Review A 7 2105–10
[5] Hoult D I and Bhakar B 1997 NMR signal reception: *Virtual photons and coherent spontaneous emission Concepts in Magnetic Resonance* 9 277–97
[6] Mallin D, Fiedler C and Vesci, *A 2018 Analysis of Mineral Oil and Glycerin through pNMR* (History Studies International Journal of History 10 241–64)